ChemPubSoc Europe

DOI: 10.1002/cssc.201903243

CHEMSUSCHEM Full Papers

Cross-linking Effects on Performance Metrics of Phenazine-Based Polymer Cathodes

Cara N. Gannett[+], Brian M. Peterson[+], Luxi Shen, Jeesoo Seok, Brett P. Fors,* and Héctor D. Abruña*[a]

Developing cathodes that can support high charge–discharge rates would improve the power density of lithium-ion batteries. Herein, the development of high-power cathodes without sacrificing energy density is reported. *N*,*N*′-diphenylphenazine was identified as a promising charge-storage center by electrochemical studies due to its reversible, fast electron transfer at high potentials. By incorporating the phenazine redox units in a cross-linked network, a high-capacity (223 mA h g^{-1}), high-voltage (3.45 V vs. Li/Li^{+}) cathode material was achieved. Optimized cross-linked materials are able to deliver reversible capacities as high as 220 mA h g^{-1} at 120 C with minimal degradation over 1000 cycles. The work presented herein highlights the fast ionic transport and rate capabilities of amorphous organic materials and demonstrates their potential as materials with high energy and power density for next-generation electrical energy-storage technologies.

Introduction

Electrification of transportation is expected to play a critical role in curbing carbon emissions and utilizing renewable energy. Recently, the U.S. Department of Energy has set an initial target of 15 min battery charging times to advance the market penetration of electric vehicles.[1] Currently, capacitors are the only electrical energy storage systems capable of stably delivering and sustaining these rates, owing to their high rates of charge storage.[2] However, since capacitors lack faradaic reactions, they have low energy densities compared with batteries, which compromise the range of electric vehicles. State-of-the-art battery materials have seen significant improvements in energy density and lifetime over the past decade. However, the diffusive nature of the energy storage processes continues to limit their rate performance.[3] Thus, it is necessary to increase the charge- and ion-transport dynamics to improve the power density of these devices.

During charge and discharge, crystalline inorganic cathodes undergo kinetically slow (de)intercalation events that limit the rate of ion diffusion. In amorphous organic materials, charge-balancing counterion transport can be dramatically enhanced owing to the relatively weak intermolecular forces in the materials.[4,5] This enables amorphous organic materials to accommodate fast ion transport, resulting in faster charging and discharging rates. However, designing amorphous organic materials that can deliver high power density without sacrificing operating voltage, capacity, or stability has proven challenging.[6–8]

Cross-linking in binders, electrolytes, and electrode materials increases resistance to dissolution, improves stability, and supports an amorphous nature to increase ion conductivity.[9–13] We hypothesized that the morphology of a redox-active polymer could be optimized by strategically tuning the cross-linking density. Cross-linking can disrupt ordering and restrict polymer mobility to ensure an open, amorphous structure even in the swelled state. Recently, we reported on a cathode material with 3,7-diamino-substituted phenothiazines as charge-storage elements.[14] In that study, cross-linking of a linear energy storage polymer led to improved stability on cycling, higher discharge capacity, and improved rate performance. Unfortunately, the material exhibited poor capacity retention on cycling, a likely consequence of polymer degradation. In an effort to better understand the effects of cross-linking, a polymer containing more stable redox centers was required. Substituted phenazines, specifically *N*,*N*′-diphenylphenazine (**1**), were identified as a promising class of charge-storage motifs through electrochemical screening/analysis of phenazine-based small-molecule analogues.

In recent years, phenazine has been identified as a promising charge-storage unit in battery cathodes, capacitors, and as a redox-flow catholyte.[15–24] Recent work on phenazine-based p-type energy materials has been led by Zhang and co-workers, who became interested in **1** for its ability to improve charge delocalization about the dihydrophenazine unit.[23,24] In collaboration with Zhou et al., they demonstrated the utility of a crystalline phenazine-based bipolar compound in a dual-ion symmetric battery with full cell capacities as high as

[a] C. N. Gannett,[+] B. M. Peterson,[+] Dr. L. Shen, J. Seok, Prof. B. P. Fors, Prof. H. D. Abruña
Chemistry and Chemical Biology, Cornell University
Ithaca, NY 14853-1301 (USA)
E-mail: brettfors@cornell.edu
hda1@cornell.edu

[+] These authors contributed equally to this work.

Supporting Information and the ORCID identification number(s) for the author(s) of this article can be found under: https://doi.org/10.1002/cssc.201903243.

This publication is part of a Special Issue focusing on "Organic Batteries". A link to the issue's Table of Contents will appear here once it is complete.

57 mA h g^{-1}. Additionally, they demonstrated the potential of a linear polymer containing phenazine units as a high-voltage cathode material delivering 65 mA h g^{-1} at a discharge rate of 5 C. However, high C-rates were not reported in either study.

Through ternary copolymerizations, we synthesized cross-linked polymers based around substituted phenazines and studied the effects of cross-linking on their electrochemical performance as amorphous cathode materials. These cross-linked phenazine-based polymers delivered energy densities competitive with those of commercial cathodes while providing dramatically enhanced power densities. By optimizing the cross-linking density in these materials, we developed a cathode material that can deliver a remarkable capacity of 220 mA h g^{-1} at 120 C with minimal capacity loss over 1000 cycles.

Results and Discussion

Electrochemical optimization of the redox storage unit

The electrochemical properties of the redox-active unit in a material can dictate many of the performance metrics of the resulting cathode, including operating voltage, cathode stability, and rate capability. Thus, careful design and electrochemical analysis of the redox unit as a small molecule can enable ideal performance in the material. Alkylation and arylation of phenazine lead to improved kinetic and thermodynamic performance metrics over unsubstituted phenazine. The *N*,*N*′-disubstituted phenazine units cycle between a neutral and dicationic state and belong to the class of so-called p-type materials.

The p-type materials typically have higher operating voltages than n-type materials (redox centers that undergo reduction and become negatively charged), which are clearly advantageous for cathode applications. Additionally, charge compensation in p-type materials is established by anion transport from the electrolyte. The smaller solvation shell of anions aids in providing higher ionic diffusion and should enable higher charge–discharge rates.[26]

Analysis of the cyclic voltammograms of phenazine and *N*,*N*′-diphenylphenazine (**1**) offers insight into their chemical and electrochemical properties. The redox processes of **1** occur at approximately 1500 mV more positive potential than those of phenazine (Figure 1). This is ideal behavior for redox units in cathodes, as it extends the operating voltage of the battery. The analysis of peak-to-peak separation, ΔE_{peak}, and the ratio of the anodic peak current to the cathodic peak current, $i_{p,a}/i_{p,c}$, of redox events sheds light on the chemical and electrochemical reversibility of the redox centers (Table 1 and Table S1 in the Supporting Information). The first redox couples, that is the transition from the neutral to the −1 state in phenazine and to the +1 state in **1**, show ΔE_{peak} values near the ideally reversible value (58 mV). For the second redox couple from the ±1 to the ±2 charge state, whereas **1** maintains a low ΔE_{peak} value of only 66 mV, the ΔE_{peak} value of phenazine increases to 216 mV, which indicates an electrochemically irreversible redox couple. Additionally, the $i_{p,a}/i_{p,c}$ value of the second redox couple in phenazine decreases with increasing scan rate, and this again corresponds to electrochemical irreversibility and potentially a coupled chemical reaction (Figure S1). Together, this suggests that materials based on **1** will show much higher operating voltages and significantly more stable cycling in cathodes than phenazine.

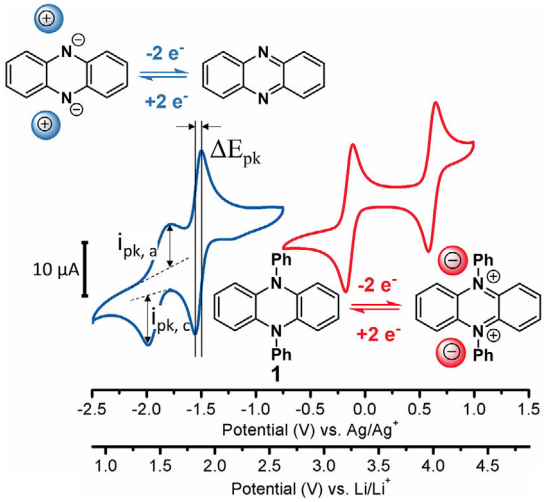

Figure 1. The neutral and reduced states of phenazine and the neutral and oxidized states of *N*,*N*′-diphenylphenazine (**1**). CV profiles at a glassy carbon electrode of 1 mM solutions of phenazine (blue) and **1** (red) obtained in 0.1 M tetrabutylammonium perchlorate (TBAP) in acetonitrile at 50 mV s^{-1}.

Table 1. Values of peak splitting, ΔE_{peak}, and standard electron-transfer rate constants, k^0, for phenazine and small molecule derivatives

Material	ΔE_{peak1} (0 → ±1) [mV]	ΔE_{peak2} (±1 → ±2) [mV]	k_1^0 [cm s^{-1}]	k_2^0 [cm s^{-1}]
phenazine	58	216	2.6×10^{-2}	–
phenazine + 50 mM TFA	107	65	1.4×10^{-2}	1.6×10^{-2}
N,*N*′-dimethylphenazine (**2**)	86	58	9.3×10^{-3}	8.5×10^{-3}
N,*N*′-diphenylphenazine (**1**)	65	66	1.1×10^{-2}	9.3×10^{-3}

Analysis of the voltammetric profiles of phenazine in the presence and absence of trifluoroacetic acid (TFA, to stabilize the reduced state through binding a proton), **1**, and *N*,*N*′-dimethylphenazine (**2**) at a Pt ultramicroelectrode was used to determine the standard electron-transfer rate constants k^0 (Figure S3). In each case, the k^0 values indicated facile and fast charge-transfer kinetics (Table 1), which therefore should not be rate-limiting even at high rates.[28] This small-molecule study ensures that the rate performance of the reported materials in battery applications will be limited by electronic conductivity or ionic diffusion through the material, and not the rate at which the redox centers can be oxidized or reduced.

Design and characterization of storage materials

When designing a redox-active polymer for electrochemical energy storage (EES), any atoms that do not contribute to faradaic processes should be limited. We hypothesized that the

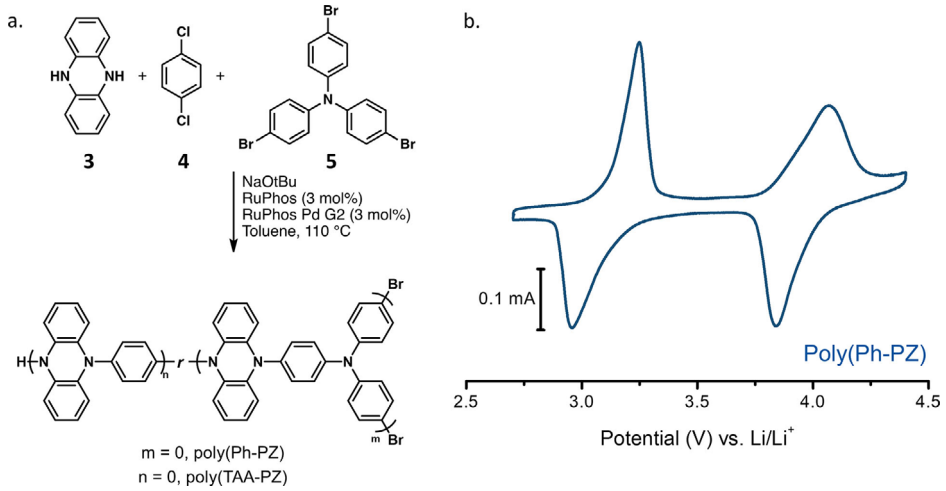

Figure 2. a) Schematic of the synthesis of poly(phenylene-5,10-dihydrophenazine) and cross-linked networks. b) CV of poly(Ph-PZ) in an Li-metal coin cell with 1 M $LiPF_6$ in EC/DEC at 2 mV s^{-1}.

core structure of **1** could be preserved and incorporated into a partially conjugated polymer framework through cross-coupling of 5,10-dihydrophenazine (**3**) and dichlorobenzene (**4**). Following a simple reduction of phenazine with sodium dithionite, the newly freed secondary amino groups of 5,10-dihydrophenazine provide excellent handles for Buchwald–Hartwig cross-coupling reactions. Cross-coupling of **3** with **4** yields poly(phenylene-5,10-dihydrophenazine) [poly(Ph-PZ)], an insoluble powder that precipitates from solution (Figure 2a). The ratio of **3** to **4** is given in Table 2, entry 1. It can be seen by comparison of the IR spectra of poly(Ph-PZ) and **1** that the polymer shares a core structure with **1** (Figure S4). As expected, the cyclic voltammogram of the material, in a lithium-metal half-cell, exhibits two one-electron oxidations, similar to the CV profile of **1** (Figure 2b).

Table 2. Reagent equivalents used in Buchwald–Hartwig cross-coupling step-growth polymerizations to obtain phenazine-based cathode materials.

Entry	Polymer	**4** (equiv)	**5** (equiv)	**6** (equiv)
1	poly(Ph-PZ)	1.0	1.0	0.0
2	poly(TAA-PZ)	1.0	0.0	0.67
3	poly(Ph-PZ)-10	1.0	0.90	0.067
4	poly(Ph-PZ)-50	1.0	0.50	0.33

Cross-linked networks were synthesized to determine the effect of cross-linking on the electrochemical properties of the cathodes. We envisaged that tris(4-bromophenyl)amine (**5**) could be copolymerized to cross-link the material (Table 2, entry 2) in order to improve stability and disrupt ordering.[5,27,28] Copolymerization of **3** with **5** results in a fully cross-linked material, namely poly(triarylamine-5,10-dihydrophenazine) [poly(TAA-PZ)], which exhibited much more resistance to dissolution in electrolyte solution than poly(Ph-PZ). This was determined by UV/Vis spectroscopy of filtered electrolyte solutions after suspending the cathode material in the electrolyte solution for one week (Figure S5). Since any solubility of the active material will result in a loss of capacity on cycling, decreasing the solubility of the material is critical to achieving near-theoretical capacity and stable cycling performance.

In our previous study on cross-linked poly(phenothiazine–dimethylphenylenediamine), we observed that, above a certain threshold of cross-linking density, rate performance declined as a result of lowered ionic transport through the material.[14] Therefore, two molar ratios of **4** and **5** were examined to determine a cross-linking density that would mitigate dissolution while retaining high ion diffusion (Table 2, entries 3 and 4). The molar ratio of poly(Ph-PZ)-10 led to a decrease in solubility in the electrolyte solution in comparison with poly(Ph-PZ) and poly(Ph-PZ)-50. Note that the degree of polymerization of the final polymer also plays a significant role in determining the solubility of the polymer. However, the cross-linked nature of the materials precludes determination of molecular weight by conventional methods.

The incorporation of cross-linker into the material was ensured by taking advantage of the relative rates of monomer cross-coupling reactions in the step-growth polymerization. Owing to the faster rate of cross-coupling of **4** with aryl bromides over aryl chlorides, we hypothesized that **6** would be more rapidly incorporated into the polymer chains than **5** to ensure cross-linked copolymers.[29,30] When the ratio of **5** to **6** is low, as in poly(Ph-PZ)-10, we expect full incorporation of the cross-linker in the polymer chains, which decreases the solubility of the polymer under battery conditions. This is supported by the elemental analysis of poly(Ph-PZ)-10, which revealed that no aryl bromide end groups were present. By contrast, elemental analysis of poly(Ph-PZ)-50 revealed 0.54% bromine content and 0.67% chlorine content. The presence of bromine in poly(Ph-PZ)-50 and the propensity of poly(Ph-PZ) for dissolution suggest that the copolymer of **3** and **5** exceeded its solubility in toluene and precipitated from the reaction solvent before **4** could be incorporated. This would leave a depleted concentration of **5** remaining in solution and result in oligomerization between **3** and **4**, as found in poly(Ph-PZ). Therefore,

whereas poly(Ph-PZ)-10 is a homogenously cross-linked material, it is more likely that poly(Ph-PZ)-50 behaves as a mixture of poly(Ph-PZ) and poly(TAA-PZ). The morphology observed by SEM provides additional support for this hypothesis (Figures S6–S8).

The crystallinity of the polymers was investigated by XRD. Diffractograms of the polymers revealed their largely amorphous character (Figure S9). At 2θ values of 10°–25°, four small, broad peaks were observed for poly(Ph-PZ) and poly(Ph-PZ)-10, indicating that some ordering is present in the polymer. As expected, this ordering was lost as the amount of **5** was increased in poly(Ph-PZ)-50 and poly(TAA-PZ). However, no melting or crystallization temperature was observed up to 200 °C by differential scanning calorimetry for any of the synthesized polymers (Figure S10). Therefore, any ordering observed by XRD is likely due to local interactions between aromatic rings and does not suggest any long-range ordering in the materials.

Coin cell design and cathode conductivity

For high-power applications, fast electron-transfer and ion-transport kinetics are necessary. To singularize the diffusion-limited rate of our materials, we aimed to minimize the rate dependence on electronic transport by making the composite conductivity sufficiently high.[3] Cathodes of each polymer were prepared as composites with active material, Super P carbon, CMK-3 mesoporous carbon, and poly(vinylidene difluoride) (PVDF) in 3:3:3:1 ratio. The partially conjugated π system in these materials is expected to enable fast electron transport through the material,[20,31,32] and the high carbon content should provide rapid charge transport through the composite, such that the electronic transport should not be limiting. When not limited electronically, the ability of the materials to transport ions should be rate-limiting during charge and discharge.

Potentiostatic electrochemical impedance spectroscopy (PEIS) and cyclic voltammetry were used to measure the charge-transfer resistance of the cathodes and the ion-diffusion coefficients, respectively (Figures S15 and S16). The fits for the charge-transfer resistance of each of the plots are listed in Table 3 (additional fitting parameters are presented in Table S2). As expected, all four polymers exhibited low-charge transfer resistance, enabling fast electron transport. The charge-transfer resistance of poly(Ph-PZ), poly(Ph-PZ)-10, and poly(Ph-PZ)-50 never exceeded 80 Ω throughout charging, indicating fast electron transfer regardless of charge state (Figure S17).

Table 3. Charge-transfer resistances, R_{ct}, and diffusion coefficients, D_{pk}, obtained from PEIS data at 2.7 V versus Li/Li$^+$ and CV data, respectively, for poly(Ph-PZ), poly(TAA-PZ), poly(Ph-PZ)-10, and poly(Ph-PZ)-50.

Polymer	R_{ct} [Ω]	D_{pk1} [cm^2 s^{-1}]	D_{pk2} [cm^2 s^{-1}]
poly(Ph-PZ)	54.0	1.6×10^{-8}	1.4×10^{-8}
poly(TAA-PZ)	100.7	4.0×10^{-9}	2.5×10^{-9}
poly(Ph-PZ)-10	57.3	1.6×10^{-8}	1.5×10^{-8}
poly(Ph-PZ)-50	49.1	5.3×10^{-9}	3.9×10^{-9}

Cyclic voltammograms of each cathode were taken over a range of scan rates. By applying the Randles–Sevcik equation, the diffusion coefficients of the PF_6^- ions through the electrode were determined. Even at high scan rates, the response remained diffusion-limited, as evidenced by the linear plot of peak current versus the square root of scan rate. The obtained diffusion coefficients of poly(Ph-PZ) and poly(Ph-PZ)-10 are of the order of 10^{-8} cm^2 s^{-1} (Table 3). The faster diffusion of PF_6^- observed in poly(Ph-PZ) and poly(Ph-PZ)-10 compared with diffusion through poly(Ph-PZ)-50 and poly(TAA-PZ) is attributed to improved ion transport in the less densely cross-linked materials. For all the polymers presented here, the values of the diffusion coefficient were orders of magnitude higher than those of commercial inorganic oxide cathodes and enable high rate capabilities while maintaining a high degree of utilization of the active material.[33–36]

Material performance in lithium half-cells

The cathodes were cycled in lithium half-cells between 1.5 and 4.3 V at 5 C (Figure 3 a), corresponding to a charge–discharge time of 12 min each, shorter than the U.S. Department of

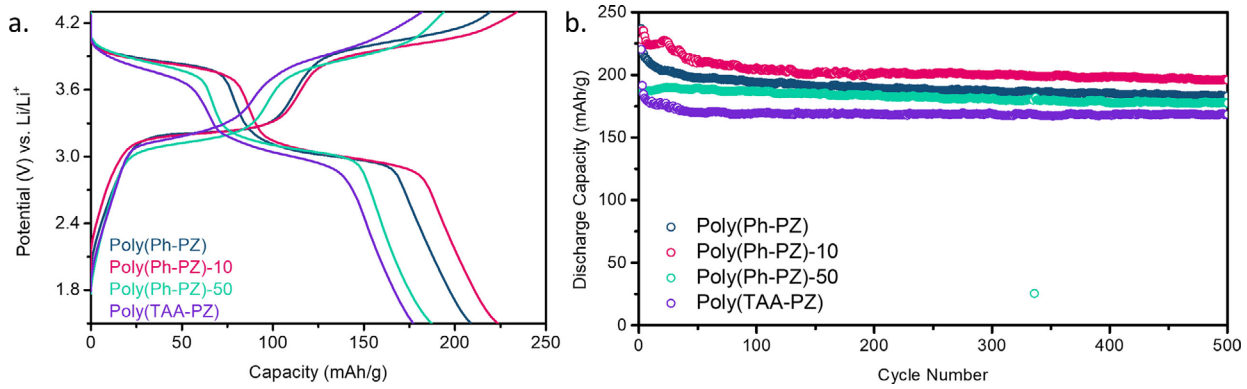

Figure 3. a) Charge–discharge profiles of the tenth cycle of poly(Ph-PZ), poly(TAA-PZ), poly(Ph-PZ)-10, and poly(Ph-PZ)-50 at 5 C. b) Discharge capacity of poly(Ph-PZ), poly(TAA-PZ), poly(Ph-PZ)-10, and poly(Ph-PZ)-50 at 5 C for 500 cycles.

Energy target charging time. Poly(Ph-PZ)-10 exhibited the highest discharge capacity of 223 mA h g^{-1}, whereas the capacity of poly(Ph-PZ) on discharge was 209 mA h g^{-1}. This improvement in capacity in poly(Ph-PZ)-10, despite its lower theoretical capacity (203 mA h g^{-1}), is attributed to the aforementioned decrease in solubility over poly(Ph-PZ). Due to the larger percentage of the inactive cross-linker, poly(Ph-PZ)-50 and poly(TAA-PZ) delivered capacities of 187 and 177 mA h g^{-1}, respectively.

Since the redox activity of the triarylamine units in the polymers falls outside the electrochemical stability window (4.5 V), they are not able to contribute any charge storage (Figure S18). Through analysis of the CV of poly(TAA-PZ), each redox peak in the CV could be attributed to oxidations of the embedded phenazine. Since there are two triarylamine units for every three phenazine units in poly(TAA-PZ), an integral ratio of 2:3 of the areas under the CV peaks would be expected if either peak was due to oxidation of the triarylamine units. However, we observed an approximately 1:1 ratio of the peak areas in the CVs of all of the polymers (Figure S19). In all cases, the experimentally measured capacities were slightly higher than the theoretical capacities of the materials owing to the additional capacity contribution from the carbon in the cathode composite (Figure S20).

Continued cycling of poly(Ph-PZ), poly(Ph-PZ)-10, poly(Ph-PZ)-50, and poly(TAA-PZ) at a C-rate of 5 illustrates the prolonged stability of each material (Figure 3b, charge capacities and coulombic efficiencies are shown in Figures S21–S24). All polymers exhibited a modest loss in capacity over the first 50 cycles. Thereafter, they retained at least 92% capacity in the 500th cycle. Notably, poly(Ph-PZ)-10 still delivered a capacity of 196 mA h g^{-1} in the 500th cycle. It is evident that optimizing cross-linking density to minimize dissolution while minimally affecting capacity is an effective strategy to design a high-energy cathode material. At an average discharge voltage of 3.45 V, poly(Ph-PZ)-10 exhibits one of the highest energy densities (approximately 770 W h kg^{-1} of active material) of all polymeric cathode materials reported.

The performance of each polymer at even more demanding discharge rates was further analyzed. Figure 4a plots capacity retention at various discharge rates as a percentage of the initial capacity of the polymer averaged over the first three cycles at 1C. When discharge rates exceeded 5C, charging rates were held constant at a C-rate of 5 to ensure a constant initial charge state and isolate the effect of rate on the discharge capacity. Evidently, all of the materials excel under demanding loads, as they maintain the majority of their capacity even when discharged at 60C. Interestingly, poly(Ph-PZ)-10 had the highest capacity retention at high rates of discharge, followed by poly(Ph-PZ)-50. All four of the polymers recovered over 90% of their capacity when the discharge rate was returned to 1C.

Owing to its high capacity, stability, and superior rate performance, poly(Ph-PZ)-10 was cycled at the extraordinary discharge rate of 120C (Figure 4b). The material delivered a capacity of 220 mA h g^{-1}, corresponding to a power density greater than 27 kW kg^{-1} when normalized to the mass of the entire cathode composite. With continued cycling, the material stabilized, as seen in the improved coulombic efficiency with cycling and the delivery of 198 mA h g^{-1} after 1000 cycles. Further tests were run to probe the performance of poly(Ph-PZ)-10 upon charging and discharging at increasing rates (Fig-

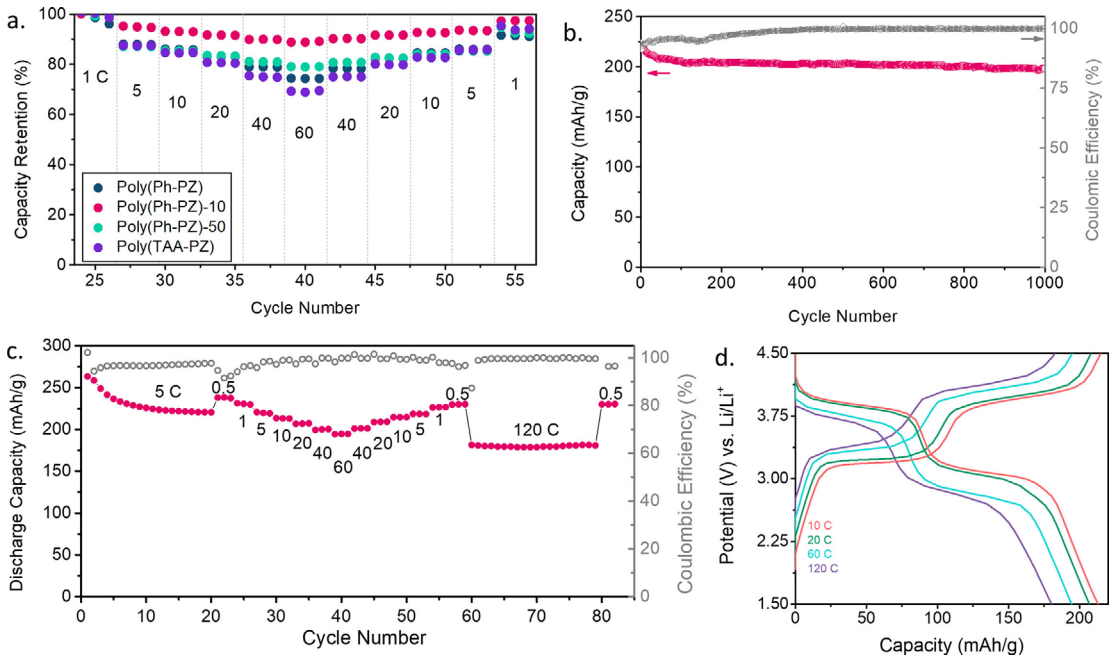

Figure 4. a) Discharge-capacity retention of poly(Ph-PZ), poly(Ph-PZ)-10, poly(Ph-PZ)-50, and poly(TAA-PZ) when discharged at increasing indicated C-rates. b) Cycling performance of poly(Ph-PZ)-10, discharged at 120C over 1000 cycles. c) Discharge capacities and coulombic efficiencies of poly(Ph-PZ)-10 charged and discharged at the denoted C-rates. d) Charge–discharge profile of poly(Ph-PZ)-10 charged and discharged at the indicated C-rates.

ure 4c). The charging voltage was increased to 4.5 V to ensure full charge at high C-rates. The material still delivered 180 mA h g^{-1} when charged and discharged at 120 C and showed excellent capacity recovery when the charge–discharge rate was returned to 0.5 C. At 120 C, poly(Ph-PZ)-10 still retains its two discrete plateaus, indicative of a faradaic charge storage mechanism (Figure 4d). These high-rate experiments illustrate the ability of amorphous materials to provide fast ion transport and enable high rates of charge–discharge. By tuning the active-mass ratio used in the composite, power and energy density can be optimized for specific applications. The energy density of a cathode composite can be driven higher by increasing the active-mass loading. Cells with 60% active material in the composite were tested at varying discharge rates. At low C-rates (0.5 C) poly(Ph-PZ)-10 was able to deliver a capacity of 182 mA h g^{-1} (Figure S28). When the cell was discharged at progressively higher C-rates (60 C), poly(Ph-PZ)-10 delivered a capacity of 143 mA h g^{-1}. Future work will focus on further understanding ionic transport through amorphous organic materials.

Performance in sodium half-cells

P-type cathode materials lend themselves to be used in alternative ion batteries. Since anions are responsible for the charge compensation of the oxidized phenazine units, materials based around this redox-active unit are largely unaffected by the metal cations in solution. Therefore, the materials presented here could be used in a range of batteries with anodes such as sodium, magnesium, and potassium without the performance of the cathode being affected. This effect was demonstrated by analyzing the CV profile of poly(Ph-PZ)-10 in a variety of electrolyte salts, as shown in Figure S29. The redox peaks of poly(Ph-PZ)-10 retain their shape and magnitude regardless of the nature of the cation in solution.

We sought to determine the efficacy of a poly(Ph-PZ)-10 cathode in a sodium half-cell, as sodium-ion batteries are touted as being a future alternative EES system to lithium ion batteries (Figure 5). Coin cells were assembled with a sodium-metal anode and a poly(Ph-PZ)-10 composite as the cathode

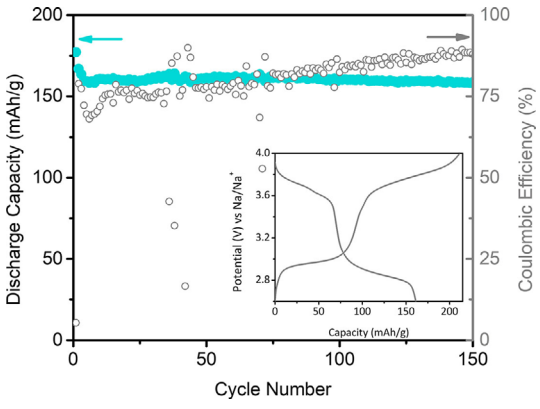

Figure 5. Cycling performance of poly(Ph-PZ)-10 in a sodium metal half-cell at 0.5 C. Inset: Charge–discharge profile of sodium metal half-cell.

with 1 M $NaPF_6$ in ethylene carbonate (EC)/diethyl carbonate (DEC) as the electrolyte. Owing to the high resistance in the sodium cell, the coin cell was tested at a relatively low C-rate. Cycling the cell at 0.5 C provided a steady discharge capacity of greater than 160 mA h g^{-1} after 100 cycles, comparable to the capacity obtained in a lithium cell. The large charging capacity in the first cycle and the poor coulombic efficiency is attributed to the incompatibility of carbonate-based electrolytes with sodium-metal deposition, which leads to increased resistance in the cell, as observed by PEIS (Figure S30).[37,38] To obtain the same results achieved in the lithium cell, each of the components of the sodium coin cell would require further optimization. Still, these results demonstrate the ability of poly(Ph-PZ)-10 to function in alternative ion batteries.

Conclusion

The performance metrics of the phenazine-based materials described herein as cathodes are among the highest reported for organic cathode materials. Careful design of cross-linked copolymer poly(Ph-PZ)-10 resulted in improved capacity, stability, and rate performance over the linear poly(Ph-PZ). At an average operating voltage of 3.45 V versus Li/Li$^+$, poly(Ph-PZ)-10 delivers 223 mA h g^{-1} and 220 mA h g^{-1} at 5 C and 120 C, respectively. Addition of the cross-linker was shown to enable a higher active-material fraction to be used in the cell while maintaining a high percentage of the material's capacity. The family of materials studied here exhibited excellent ionic transport kinetics that resulted in extraordinary capacity retention at very high C-rates. Although comparison with commercial batteries is difficult, these materials exhibit competitive energy densities while providing power densities comparable to those of commercial capacitors, demonstrating the viability of organic cathodes in EES devices. Specifically, this work demonstrates the impact of fast ionic diffusion through amorphous materials on rate capability.

Experimental Section

General synthetic procedures

General information regarding reagents can be found in the Supporting Information. *N*,*N*′-Dimethyl-5,10-dihydrophenazine and *N*,*N*′-diphenyl-5,10-dihydrophenazine were synthesized by previously reported methods.[39,40]

Fabrication of coin cells

Device measurements were conducted in CR 2032 coin cell casings, which were assembled in an argon-filled glove box with oxygen content below 1 ppm. The anode was lithium metal and the working electrode was fabricated from a slurry of 30 wt% active material (≈0.6 mg cm^{-2}), 30 wt% Super P carbon, 30 wt% CMK-3, and 10 wt% PVDF as the binder in NMP. The high-loading cathode was fabricated with 60 wt% active material, 15 wt% Super P carbon, 15 wt% CMK-3, and 10 wt% PVDF as binder. The slurries were spread onto a carbon-paper current collector by the doctor-blade method with one layer of Scotch tape. The coated electrode was dried for 2 h at 60 °C followed by 14 h at 110 °C in a

vacuum oven. A polypropylene separator (Celgard 2300) or a glass microfiber filter (GF/A, Whatman) was used as the separator between the two electrodes. The electrolyte solution was EC/DEC (1:1 *v/v*) with 1 M $LiPF_6$ (Aldrich). In cells with the Celgard separator, 60 μL of electrolyte solution was used, while 80 μL was used in the cells with the fiber-glass separators. An Arbin BT2000 battery tester was used to perform galvanostatic charge–discharge experiments on the coin cells at 25 °C.

Procedure for cyclic voltammetric experiments

Benchtop cyclic voltammetry experiments were performed in a three-compartment glass cell with medium-porosity glass frits separating the compartments. An Ag/Ag^+ reference electrode and a Pt-wire counter electrode were used. Glassy-carbon electrodes 3 mm in diameter were purchased from CH Instruments and used as working electrodes. Prior to the experiment, electrodes were polished with diamond paste and MetaDi Fluid (Buehler). All cyclic voltammetric measurements were done in 0.1 M TBAP in MeCN unless otherwise specified. The potentials in the CVs were corrected for *iR* drop by using a ferrocene reference at different scan rates.

Synthesis of 5,10-dihydrophenazine

Ethanol and deionized water were degassed by sparging with nitrogen for 30 min. Water (400 mL) and ethanol (100 mL) were added to a 1 L round-bottom flask. Phenazine (4.00 g, 22.2 mmol, 1 equiv) and sodium dithionite (46.6 g, 268 mmol, 12 equiv) were added and the solution was magnetically stirred under a nitrogen atmosphere. The reaction mixture was heated to reflux under nitrogen and the reaction allowed to proceed for 4 h. The reaction was deemed complete when no solid blue particulate material remained. The reaction mixture was allowed to cool, quickly filtered, and the residue washed with deoxygenated water to yield a light green powder (3.57 g 88% yield). The product was dried and stored under vacuum until use.

General procedure for Buchwald-Hartwig cross-coupling polymerizations

The following method was implemented for the synthesis of poly(Ph-PZ), poly(Ph-PZ)-10, poly(Ph-PZ)-50, and poly(TAA-PZ). 5,10-Dihydrophenazine, dichlorobenzene, tris(4-bromophenyl)-amine, sodium *tert*-butoxide, RuPhos ligand, and RuPhos Pd G2 precatalyst were charged to a Schlenk tube. A nitrogen atmosphere was established, and toluene was added. The reaction mixture was stirred at 110 °C for 16 h. After the reaction time, the polymer was suspended in dichloromethane and washed with water three times. After filtration, the polymer was dried at 65 °C under vacuum.

Synthesis of poly(Ph-PZ)

The general procedure for Buchwald–Hartwig cross-coupling polymerization was followed with 5,10-dihydrophenazine (273 mg, 1.50 mmol, 1 equiv), 1,4-dichlorobenzene (221 mg, 1.50 mmol, 1 equiv), RuPhos (14 mg, 0.03 mmol, 0.02 equiv), RuPhos Pd G2 precatalyst (23 mg, 0.03 mmol, 0.02 equiv), and NaO*t*Bu (346 mg, 3.6 mmol, 2.4 equiv). The polymer (357 mg) was obtained as a tan powder. IR (ATR, cm^{-1}): $\tilde{\nu}$ = 3033, 1604, 1503, 1476, 1455, 1329, 1260, 1093, 1061, 1015, 908, 817, 723, 620, 559 cm^{-1}. Elemental analysis found: C 79.63, H 4.45, N 9.64, Cl 2.71.

Synthesis of Poly(Ph-PZ)-10

The general procedure for Buchwald–Hartwig cross-coupling polymerization was followed with 5,10-dihydrophenazine (273 mg, 1.50 mmol, 1 equiv), 1,4-dichlorobenzene (198.5 mg, 1.35 mmol, 0.9 equiv), tris(4-bromophenyl)amine (48.2 mg, 0.1 mmol, 0.067 equiv), RuPhos ligand (14 mg, 0.03 mmol, 0.02 equiv), RuPhos Pd G2 precatalyst (23 mg, 0.03 mmol, 0.02 equiv), and NaO*t*Bu (346 mg, 3.6 mmol, 2.4 equiv). The polymer (394 mg) was obtained as a brown powder. IR (ATR, cm^{-1}): $\tilde{\nu}$ = 3033, 1603, 1502, 1476, 1455, 1329, 1259, 1156, 1093, 1061, 1015, 920, 817, 723, 620, 559 cm^{-1}. Elemental analysis found: C 80.50, H 4.71, N 10.36, Cl 1.19, Br 0.0.

Synthesis of poly(Ph-PZ)-50

The general procedure for Buchwald–Hartwig cross-coupling polymerization was followed with 5,10-dihydrophenazine (273 mg, 1.50 mmol, 1 equiv), 1,4-dichlorobenzene (110 mg, 0.75 mmol, 0.5 equiv), tris(4-bromophenyl)amine (241 mg, 0.5 mmol, 0.33 equiv), RuPhos ligand (14 mg, 0.03 mmol, 0.02 equiv), RuPhos Pd G2 precatalyst (23 mg, 0.03 mmol, 0.02 equiv), and NaO*t*Bu (346 mg, 3.6 mmol, 2.4 equiv). The polymer (439 mg) was obtained as a brown powder. IR (ATR, cm^{-1}): $\tilde{\nu}$ = 2079, 1605, 1499, 1479, 1455, 1333, 1280, 1259, 1156, 1093, 1061, 1015, 820, 730, 617, 555 cm^{-1}. Elemental analysis found: C 79.96, H 4.69, N 10.1, Cl 0.67, Br 0.54.

Synthesis of poly(TAA-PZ)

The general procedure for Buchwald-Hartwig cross-coupling polymerization was followed with 5,10-dihydrophenazine (273 mg, 1.50 mmol, 1 equiv), tris(4-bromophenyl)amine (482 mg, 1.0 mmol, 0.67 equiv), RuPhos ligand (14 mg, 0.03 mmol, 0.02 equiv), RuPhos Pd G2 precatalyst (23 mg, 0.03 mmol, 0.02 equiv), and NaO*t*Bu (346 mg, 3.6 mmol, 2.4 equiv). The polymer (414 mg) was obtained as a brown powder. IR (ATR, cm^{-1}): $\tilde{\nu}$ = 3028, 1606, 1497, 1479, 1456, 1310, 1282, 1256, 1158, 1099, 1060, 1013, 822, 817, 732, 616, 553 cm^{-1}. Elemental analysis found: C 76.83, H 4.59, N 9.68, Br 1.49.

Acknowledgements

This work was primarily funded by a grant to the Cornell Center for Materials Research from the NSF MRSEC program (DMR-1719875).

Conflict of interest

The authors declare no conflict of interest.

Keywords: cross-coupling · electrochemistry · N heterocycles · organic cathodes · polymers

[1] D. Howell et. al., *Enabling Fast Charging: A Technology Gap Assessment*, **2017**, DOI: https://doi.org/10.2172/1416167, accessed: September, 2019.

[2] C. Schütter, S. Pohlmann, A. Balducci, *Adv. Energy Mater.* **2019**, *9*, 1900334.
[3] R. Tian, S. H. Park, P. J. King, G. Cunningham, J. Coelho, V. Nicolosi, J. N. Coleman, *Nat. Commun.* **2019**, *10*, 1933.
[4] M. Yao, K. Kuratani, T. Kojima, N. Takeichi, H. Senoh, T. Kiyobayashi, *Sci. Rep.* **2014**, *4*, 3650.
[5] M. Armand, *Solid State Ionics* **1983**, *9–10*, 745.
[6] D. R. Nevers, F. R. Brushett, D. R. Wheeler, *J. Power Sources* **2017**, *352*, 226.
[7] B. Häupler, A. Wild, U. S. Schubert, *Adv. Energy Mater.* **2015**, *5*, 1402034.
[8] A. M. Bryan, L. M. Santino, Y. Lu, S. Acharya, J. M. D'Arcy, *Chem. Mater.* **2016**, *28*, 5989.
[9] Y. Ma, J. Ma, G. Cui, *Energy Storage Mater.* **2019**, *20*, 146.
[10] S. J. Tan, X. X. Zeng, Q. Ma, X. W. Wu, Y. G. Guo, *Electrochem. Energy Rev.* **2018**, *1*, 113.
[11] P. T. Dirlam, R. S. Glass, K. Char, J. Pyun, *J. Polym. Sci. Part A* **2017**, *55*, 1635.
[12] S. Muench, A. Wild, C. Friebe, B. Häupler, T. Janoschka, U. S. Schubert, *Chem. Rev.* **2016**, *116*, 9438.
[13] J. Lopez, D. G. Mackanic, Y. Cui, Z. Bao, *Nat. Rev. Mater.* **2019**, *4*, 312.
[14] B. M. Peterson, D. Ren, L. Shen, Y.-C. M. Wu, B. Ulgut, G. W. Coates, H. D. Abruña, B. P. Fors, *ACS Appl. Energy Mater.* **2018**, *1*, 3560.
[15] M. Lee, J. Hong, B. Lee, K. Ku, S. Lee, C. B. Park, K. Kang, *Green Chem.* **2017**, *19*, 2980.
[16] S.-Y. Yang, Y.-J. Chen, G. Zhou, Z.-W. Fu, *J. Electrochem. Soc.* **2018**, *165*, A1422.
[17] J. Wang, K. Tee, Y. Lee, S. N. Riduan, Y. Zhang, *J. Mater. Chem. A* **2018**, *6*, 2752.
[18] T. Matsunaga, T. Kubota, T. Sugimoto, M. Satoh, *Chem. Lett.* **2011**, *40*, 750.
[19] A. Hollas, X. Wei, V. Murugesan, Z. Nie, B. Li, D. Reed, J. Liu, V. Sprenkle, W. Wang, *Nat. Energy* **2018**, *3*, 508.
[20] C. Peng, G.-H. Ning, J. Su, G. Zhong, W. Tang, B. Tian, C. Su, D. Yu, L. Zu, J. Yang, *Nat. Energy* **2017**, *2*, 17074.
[21] J. Wang, C. S. Chen, Y. Zhang, *ACS Sustainable Chem. Eng.* **2018**, *6*, 1772.
[22] G. Kwon, S. Lee, J. Hwang, H. S. Shim, B. Lee, M. H. Lee, Y. Ko, S. K. Jung, K. Ku, J. Hong, K. Kang, *Joule* **2018**, *2*, 1771.
[23] G. Dai, X. Wang, Y. Qian, Z. Niu, X. Zhu, J. Ye, Y. Zhao, X. Zhang, *Energy Storage Mater.* **2019**, *16*, 236.
[24] Z. Niu, H. Wu, L. Liu, G. Dai, S. Xiong, Y. Zhao, X. Zhang, *J. Mater. Chem. A* **2019**, *7*, 10581.
[25] K. Xu, *Chem. Rev.* **2004**, *104*, 4303.
[26] A. Z. Weber, M. M. Mench, J. P. Meyers, P. N. Ross, J. T. Gostick, Q. Lui, *J. Appl. Electrochem.* **2011**, *41*, 1137.
[27] J. F. Le Nest, S. Callens, A. Gandini, M. Armand, *Electrochim. Acta* **1992**, *37*, 1585.
[28] O. Garcia-Calvo, N. Lago, S. Devaraj, M. Armand, *Electrochim. Acta* **2016**, *220*, 587.
[29] F. Barrios-Landeros, B. P. Carrow, J. F. Hartwig, *J. Am. Chem. Soc.* **2009**, *131*, 8141.
[30] B. P. Fors, S. L. Buchwald, *J. Am. Chem. Soc.* **2009**, *131*, 12898.
[31] E. Castillo-Martínez, J. Carretero-González, M. Armand, *Angew. Chem. Int. Ed.* **2014**, *53*, 5341; *Angew. Chem.* **2014**, *126*, 5445.
[32] G. P. Evans in *Advances in Electrochemical Science and Engineering* (Eds.: H. Gerischer, C. Tobias), VCH, Weinheim, **1990**, pp. 3–8.
[33] X. Wang, H. Hao, J. Liu, T. Huang, A. Yu, *Electrochim. Acta* **2011**, *56*, 4065.
[34] S. B. Tang, M. O. Lai, L. Lu, *Mater. Chem. Phys.* **2008**, *111*, 149.
[35] S. Yang, X. Wang, X. Yang, Y. Bai, Z. Liu, H. Shu, Q. Wei, *Electrochim. Acta* **2012**, *66*, 88.
[36] Y. Cui, X. Zhao, R. Guo, *Electrochim. Acta* **2010**, *55*, 922.
[37] H. Kim, J. Hong, Y. U. Park, J. Kim, I. Hwang, K. Kang, *Adv. Funct. Mater.* **2015**, *25*, 534.
[38] G. Yan, D. Alves-Dalla-Corte, W. Yin, N. Madern, G. Gachot, J.-M. Tarascon, *J. Electrochem. Soc.* **2018**, *165*, A1222.
[39] A. Sugimoto, T. Kotani, J. Tsugimoto, S. Yoneda, *J. Heterocycl. Chem.* **1989**, *26*, 435.
[40] J. C. Theriot, C.-H. Lim, H. Yang, M. D. Ryan, C. B. Musgrave, G. M. Miyake, *Science* **2016**, *352*, 1082.

Manuscript received: November 26, 2019
Revised manuscript received: December 6, 2019
Accepted manuscript online: January 23, 2020
Version of record online: ■■ ▮▮, 0000

Cross-linked cathodes: A phenazine-based polymer, namely poly(phenylene-5,10-dihydrophenazine), is cross-coupled with tris(4-bromophenyl)amine to form an amorphous cross-linked network that exhibits improved stability and rate capability when used as a high-capacity, high-voltage cathode material for lithium-ion batteries.

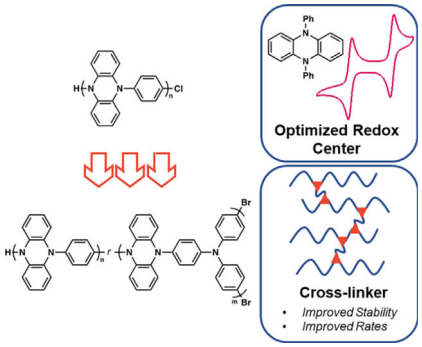

C. N. Gannett, B. M. Peterson, L. Shen, J. Seok, B. P. Fors, H. D. Abruña**

■■ – ■■

Cross-linking Effects on Performance Metrics of Phenazine-Based Polymer Cathodes

These are not the final page numbers! ↗↗